Sensors & Actuators: B. Chemical 291 (2019) 257–265

Contents lists available at ScienceDirect

Sensors and Actuators B: Chemical

journal homepage: www.elsevier.com/locate/snb

Naked-eye detection of pandemic influenza a (pH1N1) virus by polydiacetylene (PDA)-based paper sensor as a point-of-care diagnostic platform

Seong Uk Son[a,1], Seung Beom Seo[a,1], Soojin Jang[a], Jongmin Choi[c], Jae-woo Lim[a,b], Do Kyung Lee[c], Hyeran Kim[a], Sungbaek Seo[d], Taejoon Kang[a,b], Juyeon Jung[a,b,*], Eun-Kyung Lim[a,b,*]

[a] BioNanotechnology Research Center, KRIBB, 125 Gwahak-ro, Yuseong-gu, Daejeon, 34141, Republic of Korea
[b] Department of Nanobiotechnology, KRIBB School of Biotechnology, UST, 217 Gajeong-ro, Yuseong-gu, Daejeon, 34113, Republic of Korea
[c] BioNano Health Guard Research Center, KRIBB, 125 Gwahak-ro, Yuseong-gu, Daejeon, 34141, Republic of Korea
[d] Biomaterials Science, Pusan National University, 1268-50, Samnangjin-ro, Samnangjin-eup, Miryang-si, Gyeongsangnam-do, 50463, Republic of Korea

ARTICLE INFO

Keywords:
pH1N1 virus
Colorimetric detection
Paper chip
Polydiacetylene
Point-of-care diagnostic

ABSTRACT

We have developed polydiacetylene (PDA)-based colorimetric biosensor for point-of-care testing (POCT) to detect high infectious pH1N1 virus among influenza A virus with the naked eye by color change. For this purpose, we first prepared PDA-PVDF membrane by immobilizing PDA onto the PVDF membrane through photopolymerization, and then conjugated an antibody specifically binding to the influenza A virus into this membrane to form PDA-paper chips. This PDA-paper chips exhibited unique chromatic properties involving a color change from blue to red under various external conditions (temperature and pHs). Especially, we showed the color change of this paper chip in the presence of pH1N1 virus, confirming its potential as a POCT device. Furthermore, we have developed POCT systems based on PDA-paper chips by developing program, which is possible to visually detect viruses using only PDA-paper chips at a high concentration and detect and analyze them at low concentrations using both paper chips and program (App.). Further, this program will be updated to enable quantitative analysis of the virus.

1. Introduction

Numerous techniques have been developed for the rapid and sensitive detection of pandemic influenza A (pH1N1) viruses to prevent and effectively control infectious disease caused by the high infectivity of the pH1N1 virus that emerged in 2009 [1,2]. In addition, these techniques enable clinical decisions to be made near patients as point-of-care testing (POCT) so that they can reduce the time between diagnosis and treatment [3–5]. Current approaches for influenza diagnostic methods are summarized in Table S1. Especially, rapid influenza diagnostic test (LFA) and DFA (or IFA) can easily detect influenza A or B in a short time (within 4 h) based antigen detection. Other methods such as rRT-PCR and viral culture method exhibit high specificity and sensitivity, but they require labor-intensive and costly and time-consuming (48 ~ 96 h) process [6–13]. Biosensors based on colorimetric assays have great advantages in POCT: they do not require sophisticated instrumentations or technical skills for use and can be incorporated into portable sensor systems (Table S2) [14–28]. Furthermore, this method has attracted much attention because the readout can conveniently be perceived by the naked eye through chromatic changes. Noble metal nanoparticles (e.g., gold and silver) have been used in approaches to colorimetric detection. Gold nanoparticles are functionalized with a bio-receptor (e.g., antibodies and peptides) and target molecules, and their aggregation is induced by specific interactions, resulting in a colorimetric change in solution from deep red to purple [29–41]. Polydiacetylene (PDA) has recently drawn interest as a colorimetric sensing material due to its unique chromatic properties [26,15–28,42–44]. PDA exhibits blue-to-red colorimetric transitions arising from conformational changes in the PDA backbone induced by a variety of environmental perturbations, such as temperature, pH and ligand-receptor interactions. To date, PDA-based biosensors have been thoroughly investigated for the detection of

* Corresponding authors.
E-mail addresses: jjung@kribb.re.kr (J. Jung), eklim1112@kribb.re.kr (E.-K. Lim).
[1] These authors contributed equally to this work.

https://doi.org/10.1016/j.snb.2019.04.081
Received 2 September 2018; Received in revised form 15 April 2019; Accepted 16 April 2019
Available online 17 April 2019
0925-4005/

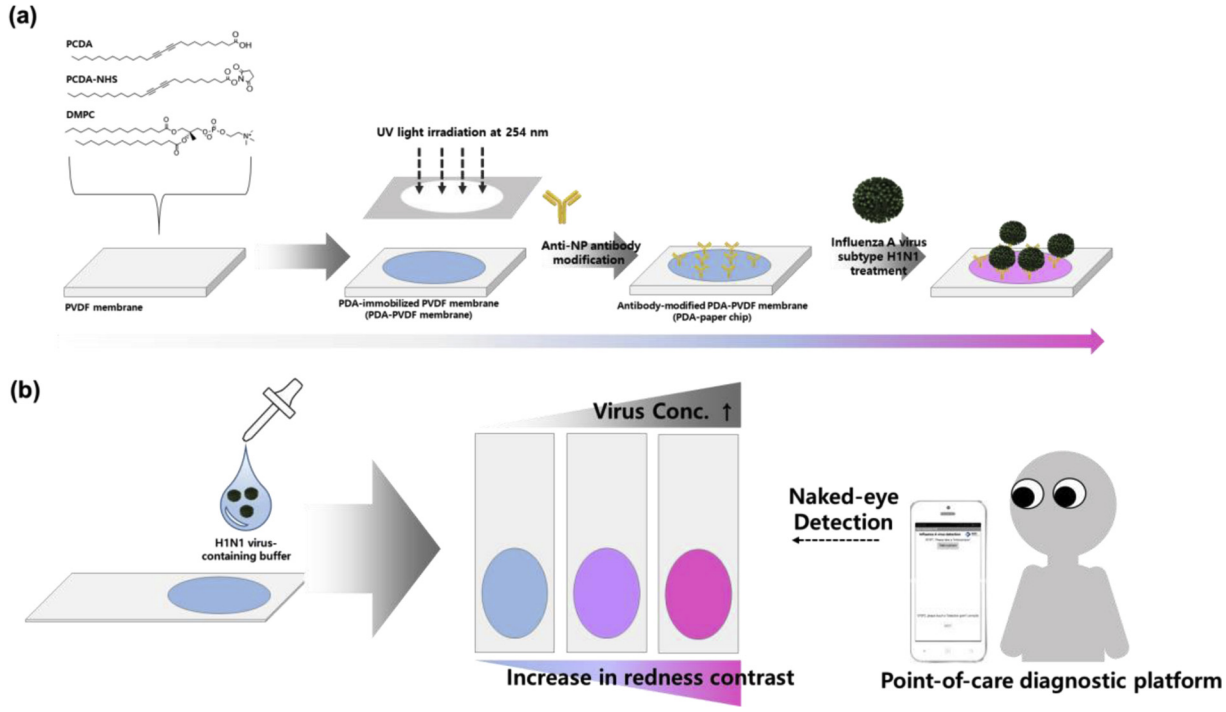

Fig. 1. (**a**) Preparation of PDA-paper chips and (**b**) their application for the colorimetric detection of influenza A (pH1N1) virus.

chemical and biological molecules such as viruses, proteins, bacteria, metal ions and organic solvents [28,44–64]. PDA-based sensors are generally categorized into two types: i) liquid-phase sensors [28,42,44–54,65,66] and ii) solid-phase sensors [67–72]. Liquid-phase sensors, which are simply PDA liposome solutions, have a few limitations, such as intrinsic aggregation upon long-term storage due to the relative instability of PDA dispersions in solution. While, because solid-phase PDA sensors use PDA molecules immobilized on a substrate in several different ways, they are ideal for development as diagnostic devices. Especially, solid-phase PDA sensors is the easiest usage and carry system that make them suitable as POCT devices. In this paper, we aimed to develop PDA-based paper chips (PDA-paper chips) that can detect influenza A (pH1N1) virus by color (naked eye) with high sensitivity (Fig. 1). We first synthesized PCDA-NHS to enable binding of an antibody to the diacetylene monomer (10,12-pentacoadiynoic acid, PCDA), and then PCDA, PCDA-NHS and a lipid were mixed with a PVDF membrane. After 1 min of UV light irradiation, a PDA-immobilized PVDF membrane (PDA-PVDF membrane) was formed by photopolymerization. Finally, PDA-paper chip was prepared by conjugating an antibody specific for influenza A virus nucleoprotein to the PDA-PVDF membrane. The color of the PDA-paper chips changed from blue to red in response to the binding events of pH1N1 virus to the chip surface. In particular, even in the presence of a nasal fluid, the pH1N1 virus could be visually detected through color change. Additionally, as soon as the pH1N1 virus was treated, PDA-paper chip was further incubated at 40 °C for 9 min to induce the thermochromic transition PDA molecules, thereby enhancing the redness contrast.

2. Experimental section

2.1. Materials

10,12-Pentacosadiynoic acid (PCDA) was purchased from Alfa Aesar (Haverhill, MA, USA). 1,2-Dimyristoyl-sn-glycero-3-phosphocholine (DMPC) was purchased from Avanti Polar Lipids (Alabaster, AL, USA). N-Hydroxysuccinimide (NHS), ethanolamine, and IgG from human serum (hIgG) were purchased from Sigma Aldrich (St. Louis, MO, USA). 1-Ethyl-3-(3-dimethylaminopropyl)carbodiimide hydrochloride (EDC) was purchased from Thermo Fisher Scientific (Waltham, MA, USA). PVDF transfer membrane (0.2 μm) was purchased from EMD Millipore (Burlington, MA, USA). Nucleoprotein antibody (anti-influenza nucleoprotein antibody) (NP) purchased from abcam (ab128193) and its cross-reactivity of the antibody against various influenza strains was performed by ELISA. All influenza strains, incldluing pandemic H1N1/09 (pH1N1) viruses (A/california/04/2009), provided by the BioNano Health Guard Research Center (H-GUARD). The Virus titers were examined by real-time PCR with a One-Step RT-PCR kit (Promega) used in accordance with the manufacturer's instructions.

2.2. Synthesis of the PDCA-NHS

First, PCDA (2.7 mmol, 1 g), *N*-hydroxysuccinimide (NHS) (2.9 mmol, 337.5 mg) and 1-Ethyl-3-(3-dimethylaminopropyl)carbodiimide (EDC) (3.2 mmol, 615 mg) were dissolved in 10 mL of dichloromethane (DCM). Then, this reactant was stirred for 4 h at room temperature. The organic solvent in this reactant was evaporated in vacuo, and the product residue was extracted ethyl acetate (EA) and distilled water. Then, the organic solvent layer was filtered by using magnesium sulfate anhydrate, and the solvent was removed in vacuo. The resulting white powder was confirmed by thin-layer chromatography (TLC, hexane/ethyl acetate, 3:1). Their chemical structures were analyzed by FT-IR spectroscopy (Bruker optics Alpha-P) (Bruker, Billerica, MA, USA) and 1H-NMR (JEOL JNM-AL 400) (JEOL, Tokyo, Japan) with DMSO-d_6 as a solvent.

2.3. Preparation of the PDA-Paper chips for pH1N1 virus detection

The powders of PCDA (0.045 mol), PCDA-NHS (0.009 mol), and DMPC (0.036 mol) were mixed with 15 mL of chloroform. The PVDF membranes were cut into square shapes using scissors. The membranes were dipped into the solution and then dried at room temperature for 6 h. Photo-irradiation of the membranes was performed with a LAB 24 UV headlamp (Dong seo, Seoul, South Korea) for 1 min, changing the membrane color to blue. After UV irradiation of the PVDF membranes at 254 nm, the membranes were incubated in a solution containing 10 μg/ml of NP antibody or human IgG as a control overnight at 4 ℃,

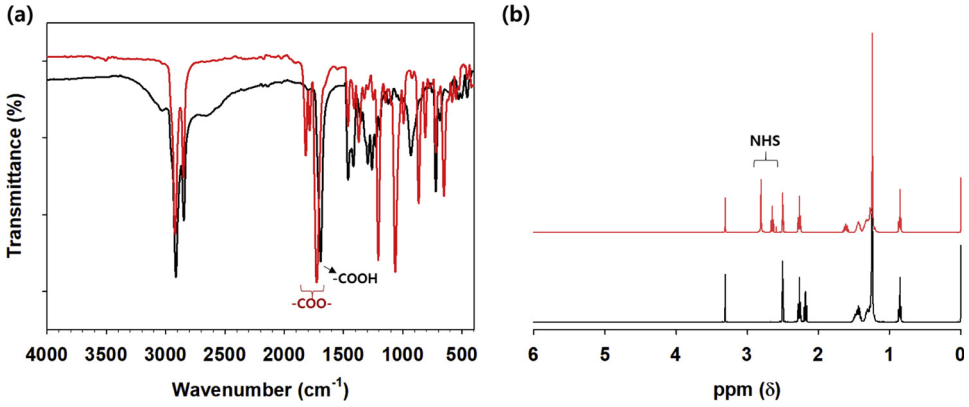

Fig. 2. (**a**) FT-IR spectra and (**b**) 1H-NMR spectra of PCDA (solid line) and PCDA-NHS (dash line).

respectively.

Next, the membranes were incubated in 18.3 nM ethanolamine for 1 h to inactivate any remaining NHS sites. After the membranes were rinsed with deionized water, they were dried in the dark. We analyzed the chemical bonds of the PVDF membrane, PDA-PVDF membranes and PDA-paper chips using an FT-IR spectrometer (Nicolet iS50) (Thermo Fisher Scientific Instrument, WI, MA, USA). PDA-paper chips should be kept in a dark place away from light and moisture light before use. Finally, PDA-paper chips were treated with the pH1N1 virus and visually observed for the detection of pH1N1 virus.

2.4. Analysis of chromatic properties of PDA-PVDF membranes under external stimuli (temperature & pH) changes

PDA-PVDF membranes were incubated at 25, 37, 40, 50, 60 and 70 ℃ for 5 min and treated with various pH solutions by adjusting with HCl (0.1 M) and NaOH (0.1 M) solution with a pH meter (METTLER TOLEDO, SevenCompact, Columbus, OH, USA) at room temperature. Then, we observed all membranes by the naked eye and obtained images for measuring their red intensity. These experiments were repeated in triplicate.

2.5. Field emission scanning Electron microscopy (FE-SEM)

The morphologies of all membrane surfaces were observed by field emission scanning electron microscopy (Hitachi, SU8230, Tokyo, Japan). The membranes were coated with platinum and studied at an accelerating voltage of 2 kV for the original PVDF membrane and 5 kV for the PDA-PVDF membrane and PDA-paper chip.

2.6. Nucleoprotein of pH1N1 virus detection using PDA-Paper chips

Before the virus test, the ability to detect nucleoproteins (NPs) using PDA-Paper chips was evaluated. NPs were prepared at various concentrations using a sample buffer (5 mM HEPES), and each solution (20 μL) was dropped on the PDA-Paper chip at room temperature to observe the color change. Bovine serum albumin (BSA) was prepared in a same manner as the control. After that, we observed their colors by the naked eye and measured their redness values. All tests were repeated in triplicate.

2.7. pH1N1 virus detection using PDA-Paper chips

First, pH1N1 viruses provided by H-GUARD were inoculated to the sample buffer (5 mM HEPES) and then diluted with the sample buffer accordance with concentrations. Then, various concentrations of pH1N1 virus-containing solution (20 μL) were treated at room temperature on the PDA-paper chips. After testing, we observed all membranes by the naked eye and then obtained images by measuring their red intensity. IgG-modified PDA-PVDF membranes were tested as a control (control Ab-paper), and this test was repeated in triplicate.

In addition, PDA-paper chip and control Ab-paper were treated with 1% nasal fluid (Lee Biosolution, Inc.) containing various concentrations of pH1N1 virus, respectively, and then their color changes were observed. Additionally, as soon as pH1N1 virus was treated, we incubated PDA-paper chips at 40 ℃ for 9 min to induce thermochromic conformational transition of PDA molecules and their colors was analyzed.

2.8. Colorimetric analysis of PDA-Paper chips

The red intensity (a*) of paper chips was measured using a spectrophotometer (CM-2600d, KONICA MINOLTA, Tokyo, Japan) and analyzed by Color Data Software (CM-S100w, KONICA MINOLTA, Tokyo, Japan). Color data are represented according to CIE (Commission International de l'Éclairage) parameter, a* for redness [73–78]. All measurements were repeated in triplicate. In addition, we have developed smartphone app. (Virus Detection) using App inventor program that can analyse virus detection using PDA-paper chips.

3. Results and discussion

3.1. Preparation and characterization of PDA-Immobilized PVDF membrane (PDA-PVDF membrane)

As previously reported, we conjugated NHS ester to PCDA via an esterification to synthesize PCDA-NHS as an antibody binding site and confirmed their chemical structures by both FT-IR and ^{1}H-NMR spectra. PCDA exhibited carboxylic acid stretching (−COOH) at 1698 cm^{-1}, whereas PCDA-NHS did not show this peak. Furthermore, a new peak at 1729 cm^{-1} corresponding to the ester bond (−COO−) was observed for PCDA-NHS (Fig. 2(a)) [28,67,79,80]. In the ^{1}H-NMR spectra, PCDA-NHS showed an NHS peak at 2.8 ppm, and this peak was absent in PCDA (Fig. 2(b)) [28]. PDA-PVDF membranes for PDA-paper chips capable of virus detection were fabricated as described in the materials and methods. A mixture of PCDA, PCDA-NHS and a lipid (1,2-dimyristoyl-sn-glycero-3-phosphocholine, DMPC) (5:1:4 M ratio) was added to a PVDF membrane to form self-assembled diacetylene vesicles. The immobilization conditions were selected through optimization of various parameters [28,37,46,48,50,53,77]. This PDA-PVDF membrane comprised lipid (DMPC) monolayers as a biomimetic surface for the docking and insertion of lipophilic and membrane active species and PDA as a module responsible for the generation of color signals. After that, UV light was irradiated for 1 min to form PDA-PVDF membranes, which exhibited a blue color. Although PDA was embedded in PVDF membrane, it was systematically perturbed by increasing the pH and temperature (Fig. 3). As shown in Fig. 3, the color of this PDA-PVDF

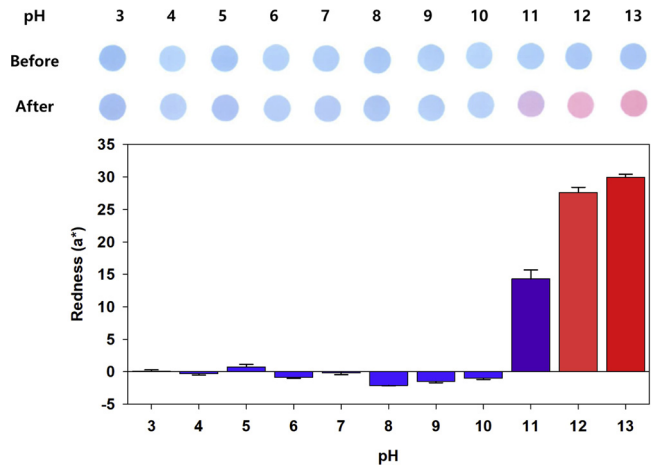

Fig. 3. Color transition images and redness (a*) values of PDA-PVDF membrane after changes in pH values.

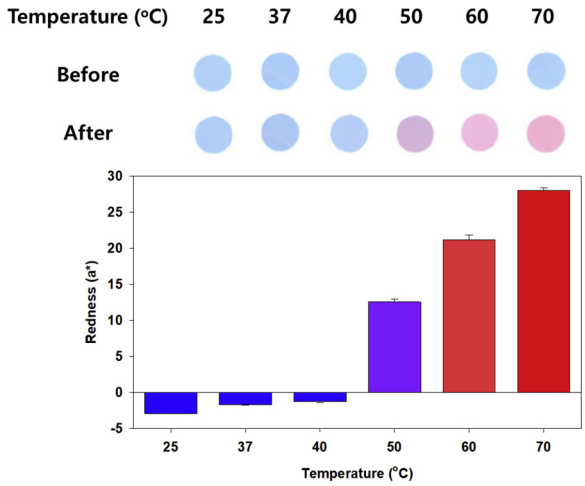

Fig. 4. Color transition images and redness (a*) values of PDA-PVDF membrane after changes in temperature.

membrane was blue under acidic and neutral conditions (pH 3 ~ 9) and gradually changed to red under basic conditions (pH 10 ~ 13), consistent with increasing trend in redness(a*) values [39]. Under basic conditions, OH- ions abstracted the carboxylic protons of PDA, leading to a systematic increase in the content of negatively charged carboxylate groups. The segments of PDA were rearranged owing to the interruption of the dispersion interaction between the alkyl tails by the strong electrostatic repulsive force between the carboxylate groups. Therefore, compared to acidic and neutral conditions, a pH above 11 (strongly basic conditions) could cause a red intensity (redness value) increase of more than 15 redness value. The PDA-PVDF membrane also exhibited a color transition from blue to red with increasing temperature. As the temperature increased, the dynamics of all segments within PDA increased, causing the PDA segments to be rearranged by weakening inter- and intra-chain interactions within PDA, which in turn altered the electronic state of the conjugated backbone. Therefore, the HOMO-LUMO energy gap of perturbed PDA was widened upon increasing the temperature, leading to a color change from blue to red (Fig. 4) [28]. We visually confirmed the color change with increasing temperature and found that the corresponding redness (a*) value also increased. These results confirmed that PCDA was photopolymerized in the PVDF membrane serving as the support to form PDA, resulting in chromatic properties. As previously mentioned, the dynamic of PDA segments was facilitated by the temperature increases. PDA segments were rearranged by weakening inter- and intra-chain interactions within this membrane, induced in turn change of the electronic state of conjugated backbone. Their HOMO-LUMO energy gap was widen when the temperature rises, leading to the color transition from blue to red [28]. On this basis, we attempted to develop a system capable of visual detection of viruses by introducing an antibody into the PDA-PVDF membrane.

3.2. Preparation of antibody-modified PDA-PVDF membranes (PDA-Paper chips)

For the visual detection of influenza A virus, especially pH1N1 virus, an NP antibody (anti-influenza nucleoprotein antibody) specific for influenza A virus nucleoprotein was introduced into the PDA-PVDF membranes, forming antibody-modified PDA-PVDF membranes (PDA-paper chips). In particular, to prevent antibody damage by UV light, we irradiated this membrane with UV light before NP antibody binding [66]. Nevertheless, the PDA-PVDF membranes maintained their blue color regardless of antibody binding. The chemical composition of the membranes was investigated by FT-IR analysis. All membranes displayed characteristic absorption bands at 1400 and 1180 cm^{-1}, corresponding to the -CF_2 stretching vibration of the PVDF membrane (Fig. 5 (a)) [67,79,80]. After PDA was coated on the PVDF membrane, the weak absorption bands of C═O stretching vibrations associated with the carboxylic acids in PCDA emerged at 1735 cm^{-1} (Fig. 5 (b)). In particular, C═N and C═O stretching vibrations of the amide bonds appeared only in FT-IR spectrum of PDA-paper chip (red line), indicating that the antibodies were well conjugated with the PDA-PVDF membrane (Fig. 5(b)). In addition, the pore structures on the membrane surface were observed by SEM imaging (Fig. 6) [81]. The pore structure and size of the PDA-PVDF membrane before and after UV irradiation did not obviously change compared to those of the bare PVDF membrane (Fig. 6(a)-(c)). On the other hand, because the membrane pores were blocked by conjugated antibodies of high molecular weight, narrowed pores were observed after antibody modification (Fig. 6(d)).

3.3. Influenza a (pH1N1) virus detection using PDA-Paper chips

Most PDA sensors have been developed as chemo-sensors or small-molecule (e.g., peptide and protein) detection sensors [37,45–47,55–58,65]. We attempted to develop PDA-paper chips that can detect whole viruses (influenza A virus) visually. First, we evaluated the ability to detect influenza A NPs at various concentrations using PDA-paper chips (Fig. 7). As shown in Fig. 7(a), as NPs concentrations on the PDA-paper chips increases, the blue paper chip gradually turned to red color and the redness value tends to increases. On the other hand, there was little change in color when treated with BSA. These results showed usability as a virus detection system using this PDA-paper chip. We dropped pH1N1 virus on PDA-Paper chip. After 3 h incubation at room temperature, the color changes in PDA-paper chips were monitored and scanned. Additionally, we measured redness intensities by spectrophotometer of this paper chips for their quantitative analysis. Human IgG antibody instead of NP antibody was used as a control. The color of the NP antibody-modified PDA-paper chip was blue in the absence of virus (0 $TCID_{50}$/mL); however, it gradually turned to red as the virus concentration increased, because colorimetric transitions within PDA matrix through perturbations induced by interaction between nucleoprotein (NP) of pH1N1 virus and NP antibody onto the PDA surface (Fig. 8(a)). Under 5×10^4 $TCID_{50}$ or more, the color of our paper chip was confirmed to be clearly changed from blue to purple and red. Importantly, the redness (a*) values were also slightly changed in accordance with their image change (Fig. 8(b)). Although there is no significant difference in the images, the redness (a*) value of PDA-paper chip at low concentrations of 5×10^3 $TCID_{50}$ was measured to be 2-folds more redness than the control (control Ab-paper). While control Ab-paper color was hardly change (Fig. 8(a)). Additionally, to increase detectability and reduce detection time, we

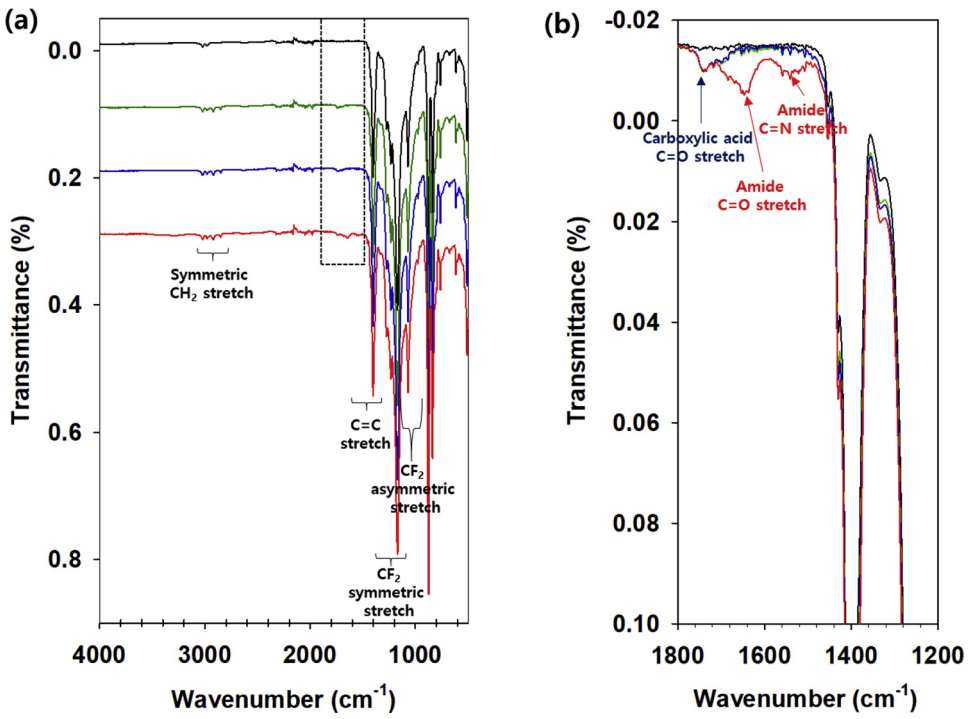

Fig. 5. (**a**) FT-IR spectra of a PVDF membrane (black), PDA-PVDF membranes before (green) and after (blue) UV irradiation and NP antibody-modified PDA-PVDF membranes (PDA-paper chips) (red) and (**b**) an enlarged graph within the range of the dashed line in (a). (For interpretation of the references to colour in this figure legend, the reader is referred to the web version of this article).

kept this paper chips in 40 °C incubator for 9 min after pH1N1 virus treatment. As shown in Fig. 4, the color of this paper chips remained unchanged with blue color at 40 °C. Although this temperature did not directly affect the thermochromic blue-to-red shift of PDA molecules, we judged that external temperature change in the PDA-paper chip could weaken the stability of PDA backbone perturbed by virus binding, thereby triggering the perturbation and increasing the redness contrast [42,44,49,66]. As our expected, the detection sensitivity of PDA-paper chips was increased overall (Figure S1). Especially, the red intensity of PDA-paper chip was increase in 10^5 $TCID_{50}$ of pH1N1 virus, and it was clearly visible. Compared with that of Fig. 8, its color was definitely changed from blue to purple, in the presence of 10^4 $TCID_{50}$ of pH1N1 virus, and it was distinctly distinguished with the naked eye (Figure S1(a)). As well, overall redness (a*) values of PDA-Paper chips were increased (Figure S1(b)). However, colors of control Ab-paper were maintained blue regardless of virus concentrations. NP antibody we used exhibited binding specificity for most influenza A viruses, including pH1N1 strain, and showed high selectivity in H3N2 virus (A/Human seasonal/10/2007) (Figure S2). As well, this assay also markedly changed from blue to red to be visible to the naked eye after H3N2 virus detection (5×10^4 $TCID_{50}$). This PDA-paper chip was able to detect H3N2 virus with high sensitivity compared with to pH1N1 virus

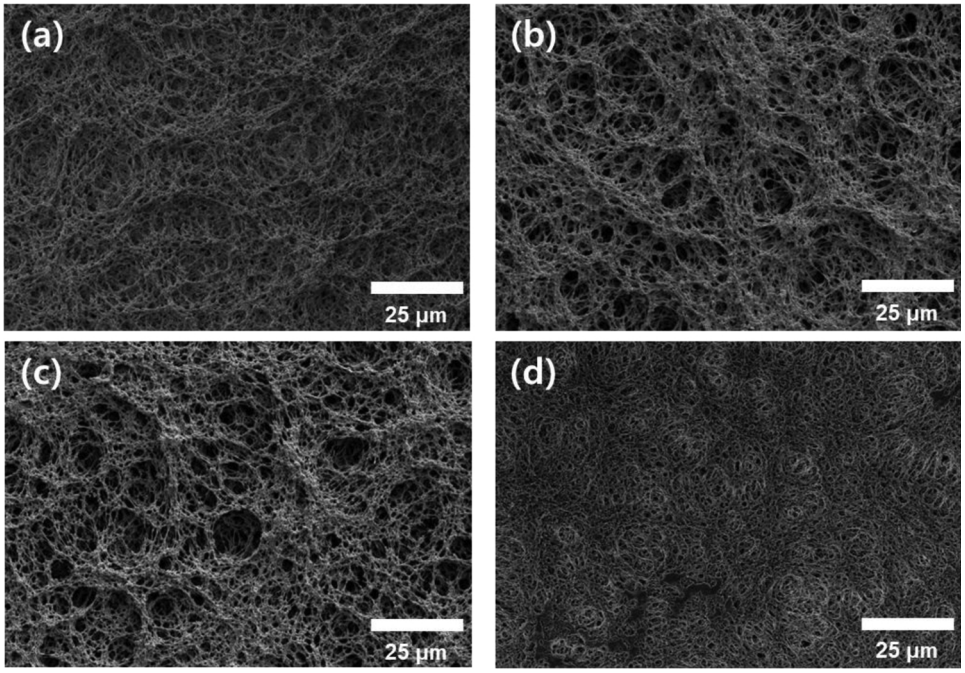

Fig. 6. SEM images of (**a**) PVDF membrane, PDA-PVDF membranes (**b**) before and (**c**) after UV laser irradiation for 1 min, and (**d**) antibody-modified PDA-PVDF membranes (PDA-paper chips) (Scale bar: 25 μm).

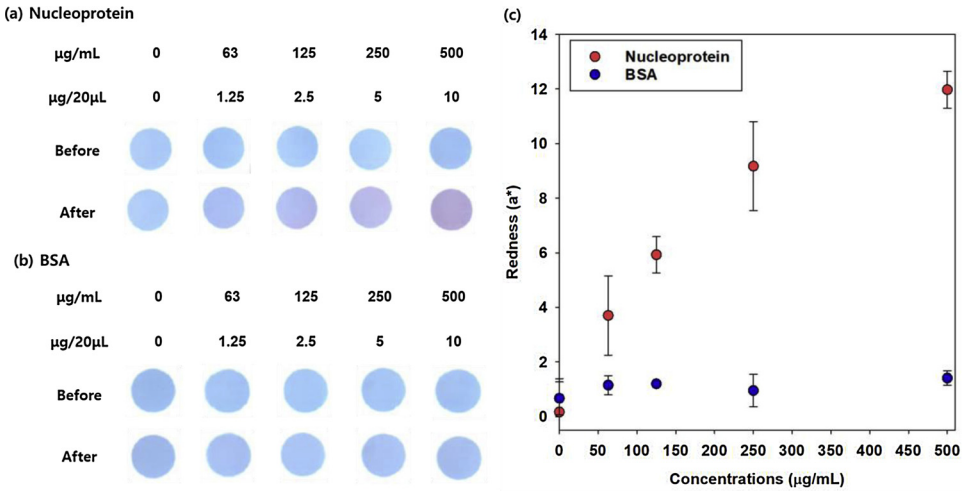

Fig. 7. Color transition images of (a) nucleoprotein and (b) bovine serum albumin (BSA) detection using PDA-paper chip at room temperature, respectively, and (c) their redness (a*) values after detection (nucleoprotein: red triangle and BSA: blue circle). (For interpretation of the references to colour in this figure legend, the reader is referred to the web version of this article).

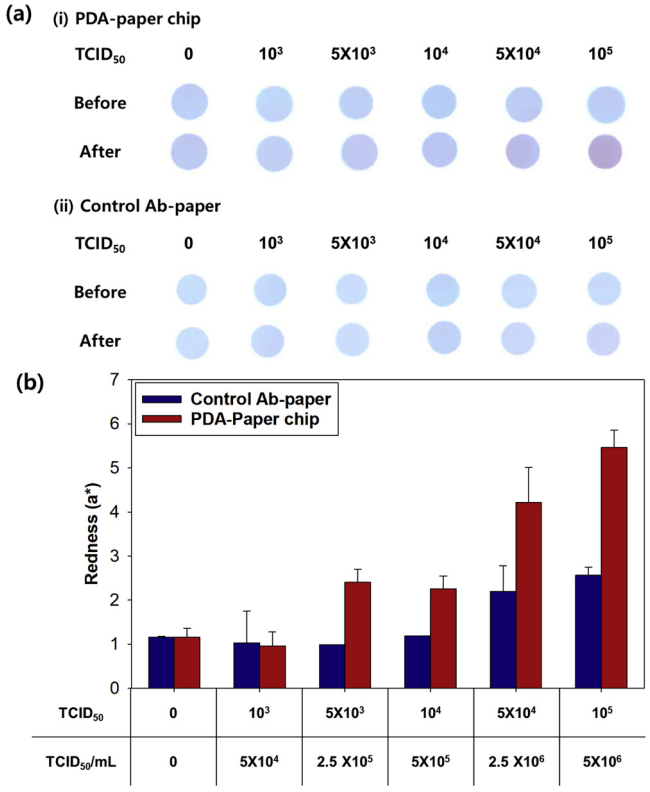

Fig. 8. (a) Color transition images of (i) PDA-paper chip and (ii) control Ab-paper after treatment with various concentrations of pH1N1 virus for 3 h at room temperature, respectively, and (b) their redness (a*) values after treatment with various concentrations of pH1N1 virus (PDA-paper chip: dark red and control Ab-paper: dark blue). (For interpretation of the references to colour in this figure legend, the reader is referred to the web version of this article).

detection, which is similar tendency to the virus specificity result of the antibody (Figure S3). Depending on the application of various antibodies, this PDA-paper chip can detect a wide variety of targets (viruses). It is important to make sure that the system works well in clinical settings. We tested whether color change of PDA-paper chips occurred by using 1% nasal fluid spiked with pH1N1 virus. As shown in Fig. 9, its color slightly changed red at the high concentration of pH1N1 virus treatment (10^4 ~ 10^5 $TCID_{50}$), but control chips were well-maintained the blue color without color change in most conditions despite the presence of nasal fluid. Of course, it needs a further improvement that its color change was not visually confirm at low concentration

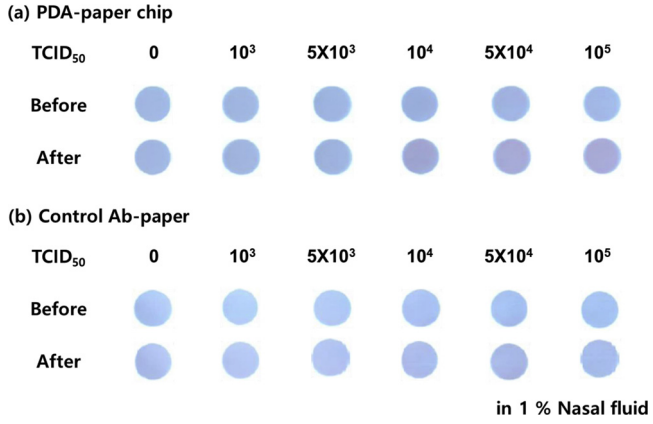

Fig. 9. Color transition images of (a) PDA-paper chips and (b) control Ab-paper after treatment with various concentration of pH1N1 in 1% nasal fluid for 3 h at room temperature, respectively.

(5×10^3 $TCID_{50}$) compared with the results in the absence of nasal fluid (Fig. 8). The characteristics (limit of detection, detection time, etc.) of biosensors for the visual detection (naked eye observation) of influenza viruses are various (Table S2). The detection sensitivity of PDA-paper chip was not yet enough to detect the influenza virus with naked eyes observation compared to other methodologies [21–28]. To complement the sensitivity of visual detection, we further developed smartphone app. (Virus Detection) that can analyse virus detection using PDA-paper chips. Importantly, since the camera specifications and detection environment (light brightness and color) are different for each smart phone, background setting should be required (Fig. 10). This program was analysed based on the RGB values of the touched part of the paper chips and their ratios. In the first step, after running this app., the PDA-paper chip is photographed (press “Take a picture” button) before virus detection (Paper chips before virus treatment) and touched the center of the detection area (detection point) correctly (Fig. 10(a)-(b)). If you do not touch the blue PDA paper chip correctly, the NEXT button will not be activated. And then press “NEXT” button to set it to the background of this chip (Fig. 10(b)-(c)). And then, after sample treatment on this chip, take a picture of this chip again and touch the detection part to analyze it (Fig. 10(d)). If there is virus on PDA-paper chip, “Virus detected” appears; otherwise, “No virus detected” appears (Fig. 10(d)) [82,83]. Thus, this PDA-paper chip can be visually detected viruses at a certain concentration or more (high concentration) and can be detected and analyzed with the help of this program with a lower concentration (low concentration). Commercially available rapid influenza diagnostic kits can detect an average 10^5 $TCID_{50}$ virus

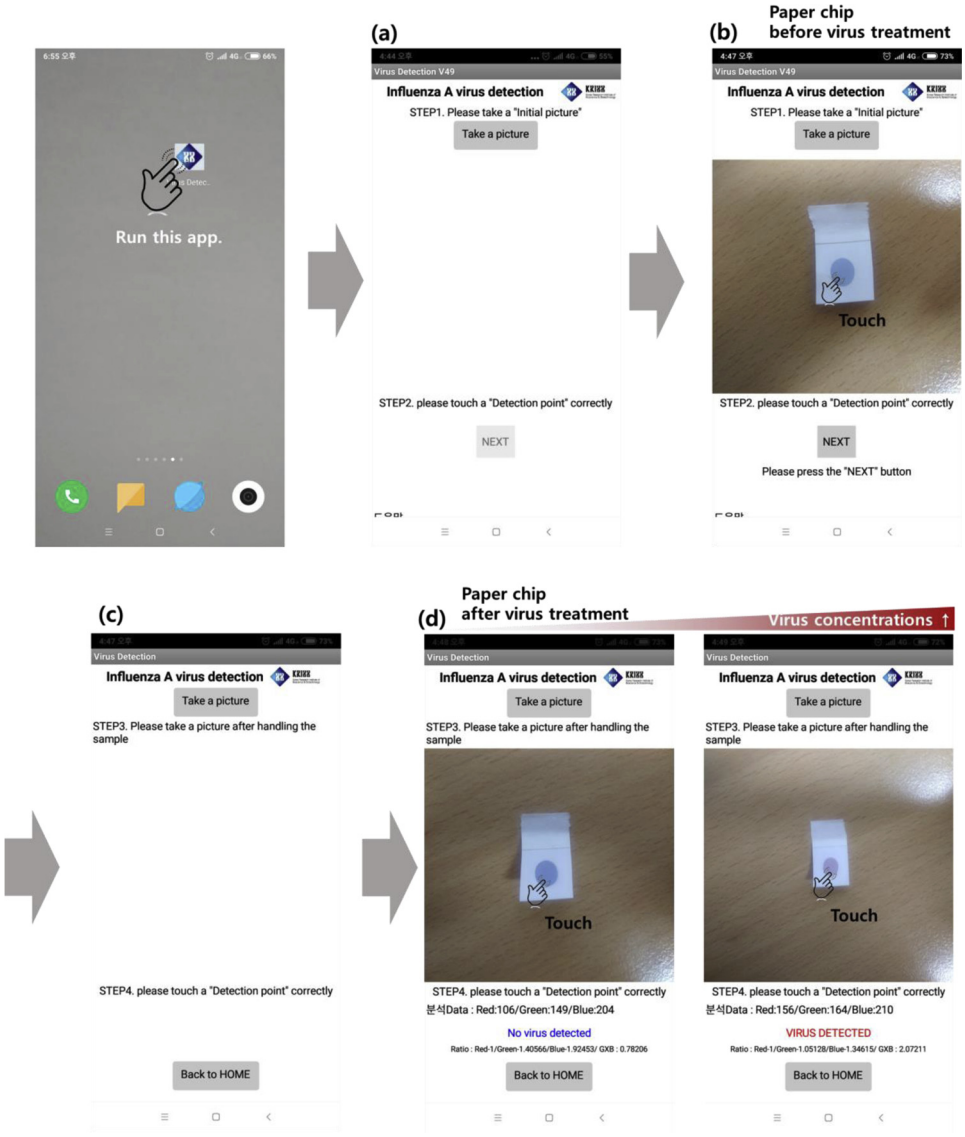

Fig. 10. Smartphone-based Virus sensing procedure. Each panel shows the smartphone screen of (a) start-up screen, (b) background setting of PDA-paper chip before virus treatment, (c) screen after background setting, and (d) analysis process after virus treatment. (The finger image does not appear on the actual screen.).

concentrations without reading device, and up to 10^4 $TCID_{50}$ when using reading device [84]. It was confirmed that PDA-paper chip is capable of visual detection of pH1N1 virus through color change from 5×10^3 ~ 10^4 $TCID_{50}$ viruses. Of course, this system needs to be improved in order to detect viruses with distinct color changes at low concentrations. Nevertheless, based on its detection sensitivity up to now, it is considered that this PDA-paper chip can also be applied to clinical situations when compared with other rapid kits.

4. Conclusions

We developed PDA-paper chips that can visually detect pH1N1 virus by changing color. These chips exhibited unique chromatic properties in accordance with external conditions (temperature and pHs). PDA-paper chips showed blue-to-red color changes in the presence of various concentrations of pH1N1 virus by interaction with influenza A virus nucleoprotein (NP) and NP antibodies on this paper chips. However, its detection sensitivity is still insufficient for clinical applications and needs to be further improve. To overcome the current shortcomings, we have developed smartphone app (i.e., program). We could visually detect high concentration of viruses using only PDA-paper chips and detect and analyze them at low concentrations using both paper chips and program (App.). Further, this program will be updated to enable quantitative analysis of the virus.

Acknowledgments

This work was supported by the BioNano Health-Guard Research Center funded by the Ministry of Science and ICT (MSIT) of Korea as the Global Frontier Project (H-GUARD_2014M3A6B2060507 and H-GUARD_2013M3A6B2078950), the Bio & Medical Technology Development Program of the National Research Foundation of Korea (NRF) funded by MSIT (NRF-2018M3A9E2022821), the Basic Science Research Program of the NRF funded by the MSIT (NRF-2018R1C1B6005424), and KRIBB Research Initiative Program.

Appendix A. Supplementary data

Supplementary material related to this article can be found, in the online version, at doi:https://doi.org/10.1016/j.snb.2019.04.081.

References

[1] V.G. Gorbulev, J.V. Kozlov, A.G. Kurmanova, A.A. Bayev, A.A. Shilov, V.M. Zhdanov, On the Origin of the H1N1 A-USSR-90-77 Influenza Virus, J. Gen. Virol. 56 (1981) 437–440.

[2] H.-O. Kim, W. Na, M. Yeom, J. Choi, J. Kim, J.-W. Lim, et al., Host cell mimic polymersomes for rapid detection of highly pathogenic influenza virus via a viral fusion and cell entry mechanism, Adv. Funct. Mater. 28 (2018) 1800960–1800969.

[3] J.R. Choi, K.W. Yong, R. Tang, Y. Gong, T. Wen, H. Yang, et al., lateral flow assay based on paper-hydrogel hybrid material for sensitive point-of-Care detection of dengue virus, Adv. Healthc. Mater. 6 (2017).

[4] G.A. Posthuma-Trumpie, J. Korf, Av. Amerongen, Lateral flow (immuno)assay: its strengths, weaknesses, opportunities and threats. A literature survey, Anal. Bioanal. Chem. 393 (2009) 569–582.

[5] E.K. Lim, T. Kim, S. Paik, S. Haam, Y.M. Huh, K. Lee, Nanomaterials for theranostics: recent advances and future challenges, Chem. Rev. 115 (2015) 327–394.

[6] C.-S. Lee, The diagnosis and treatment of influenza, J. Korean Med. Assoc. 53 (2010) 43–51.

[7] A. Ruest, S. Michaud, S. Deslandes, E.H. Frost, Comparison of the Directigen flu A+B test, the QuickVue influenza test, and clinical case definition to viral culture and reverse transcription-PCR for rapid diagnosis of influenza virus infection, J. Clin. Microbiol. 41 (2013) 3487–3493.

[8] M. Pérez-Ruiz, R. Yeste, M.J. Ruiz-Pérez, A. Ruiz-Bravo, M. de la Rosa-Fraile, J.M. Navarro-Marí, Testing of diagnostic methods for detection of influenza virus for optimal performance in the context of an influenza surveillance network, J. Clin. Microbiol. 45 (2007) 3109–3110.

[9] S. Kumar, K.J. Henrickson, Update on influenza diagnostics: lessons from the novel H1N1 influenza A pandemic, Clin. Microbiol. Rev. 25 (2012) 344–361.

[10] D.R. Peaper, M.L. Landry, Rapid diagnosis of influenza: state of the art, Clin. Microbiol. Rev. 34 (2014) 365–385.

[11] D. Sivaraman, P. Biswas, L.N. Cella, M.V. Yates, W. Chen, Detecting RNA viruses in living mammalian cells by fluorescence microscopy, Trends Biotechnol. 29 (2011) 307–313.

[12] A.C. Hurt, A.W. Hampson, F.Y. Wong, D. Lamb, I.G. Barr, R. Alexander, A comparison of a rapid test for influenza with laboratory-based diagnosis in a paediatric population, Commun. Dis. Intell. Q. Rep. 29 (2005) 272–276.

[13] C. Chartrand, M.M. Leeflang, J. Minion, T. Brewer, M. Pai, Accuracy of rapid influenza diagnostic tests: a meta-analysis, Annal. Intern. Med. 156 (2012) 500–511.

[14] A.C. Hurt, C. Baas, Y.M. Deng, S. Roberts, A. Kelso, I.G. Barr, Performance of influenza rapid point-of-care tests in the detection of swine lineage A(H1N1) influenza viruses, Influenza Other Respir. Viruses 3 (2009) 171–176.

[15] A. Nougairede, L. Ninove, C. Zandotti, X. de Lamballerie, C. Gazin, M. Drancourt, et al., Point of care strategy for rapid diagnosis of novel A/H1N1 influenza virus, PLoS One 5 (2010) e9215.

[16] K. Guk, J.O. Keem, S.G. Hwang, H. Kim, T. Kang, E.K. Lim, et al., A facile, rapid and sensitive detection of MRSA using a CRISPR-mediated DNA FISH method, antibody-like dCas9/sgRNA complex, Biosens. Bioelectron. 95 (2017) 67–71.

[17] E.K. Lim, K. Guk, H. Kim, B.H. Chung, J. Jung, Simple, rapid detection of influenza A (H1N1) viruses using a highly sensitive peptide-based molecular beacon, Chem. Commun. (Camb.) 52 (2016) 175–178.

[18] S.G. Hwang, K. Ha, K. Guk, D.K. Lee, G. Eom, S. Song, et al., Rapid and simple detection of Tamiflu-resistant influenza virus: development of oseltamivir derivative-based lateral flow biosensor for point-of-care (POC) diagnostics, Sci. Rep. 8 (2018) 12999–13010.

[19] J. Moon, J. Byun, H. Kim, E.K. Lim, J. Jeong, J. Jung, et al., On-site detection of aflatoxin B1 in grains by a palm-sized surface plasmon resonance sensor, Sensors Basel (Basel) 18 (2018) 598–606.

[20] W. Zhao, M.A. Brook, Y. Li, Design of gold nanoparticle-based colorimetric biosensing assays, Chembiochem 9 (2008) 2363–2371.

[21] T.T. Le, P. Chang, D.J. Benton, J.W. McCauley, M. Iqbal, A.E. Cass, Dual recognition element lateral flow assay toward multiplex strain specific influenza virus detection, Anal. Chem. 89 (2017) 6781–6786.

[22] N. Wiriyachaiporn, H. Sirikett, W. Maneeprakorn, T. Dharakul, Carbon nanotag based visual detection of influenza A virus by a lateral flow immunoassay, Microchim. Acta 184 (2017) 1827–1835.

[23] C. Lin, Y. Guo, M. Zhao, M. Sun, F. Luo, L. Guo, et al., Highly sensitive colorimetric immunosensor for influenza virus H5N1 based on enzyme-encapsulated liposome, Anal. Chim. Acta 963 (2017) 112–118.

[24] T.T. Le, B. Adamiak, D.J. Benton, C.J. Johnson, S. Sharma, R. Fenton, et al., Aptamer-based biosensors for the rapid visual detection of flu viruses, Chem. Commun. (Camb.) 50 (2014) 15533–15536.

[25] S.R. Ahmed, J. Kim, T. Suzuki, J. Lee, E.Y. Park, Enhanced catalytic activity of gold nanoparticle-carbon nanotube hybrids for influenza virus detection, Biosens. Bioelectron. 85 (2016) 503–508.

[26] A. Reichert, J.O. Nagy, W. Spevak, D. Charych, Polydiacetylene liposomes functionalized with sialic acid bind and colorimetrically detect influenza virus, J. Am. Chem. Soc. 117 (1995) 829–830.

[27] S. Seo, J. Lee, E.J. Choi, E.J. Kim, J.Y. Song, J. Kim, Polydiacetylene liposome microarray toward influenza a virus detection: effect of target size on turn-on signaling, Macromol. Rapid Commun. 34 (2013) 743–748.

[28] S. Song, K. Ha, K. Guk, S.G. Hwang, J.M. Choi, T. Kang, et al., Colorimetric detection of influenza A (H1N1) virus by a peptide-functionalized polydiacetylene (PEP-PDA) nanosensor, RSC Adv. 6 (2016) 48566–48570.

[29] J.D. Driskell, C.A. Jones, S.M. Tompkins, R.A. Tripp, One-step assay for detecting influenza virus using dynamic light scattering and gold nanoparticles, Analyst 136 (2011) 3083–3090.

[30] Y. Jiang, H. Zhao, Y. Lin, N. Zhu, Y. Ma, L. Mao, Colorimetric detection of glucose in rat brain using gold nanoparticles, Angew. Chem. Int. Ed. Engl. 49 (2010) 4800–4804.

[31] K. Kalidasan, J.L. Neo, M. Uttamchandani, Direct visual detection of Salmonella genomic DNA using gold nanoparticles, Mol. Biosyst. 9 (2013) 618–621.

[32] J.R. Kalluri, T. Arbneshi, S. Afrin Khan, A. Neely, P. Candice, B. Varisli, et al., Use of gold nanoparticles in a simple colorimetric and ultrasensitive dynamic light scattering assay: selective detection of arsenic in groundwater, Angew. Chem. Int. Ed. 121 (2009) 9848–9851.

[33] B. Kong, A. Zhu, Y. Luo, Y. Tian, Y. Yu, G. Shi, Sensitive and selective colorimetric visualization of cerebral dopamine based on double molecular recognition, Angew Chem Int Ed, Engl 50 (2011) 1837–1840.

[34] A.T. Lam, J. Yoon, E.O. Ganbold, D.K. Singh, D. Kim, K.H. Cho, et al., Colloidal gold nanoparticle conjugates of gefitinib, Colloids Surf. B Biointerfaces 123 (2014) 61–67.

[35] C. Lee, M.A. Gaston, A.A. Weiss, P. Zhang, Colorimetric viral detection based on sialic acid stabilized gold nanoparticles, Biosens. Bioelectron. 42 (2013) 236–241.

[36] Y. Liu, L. Zhang, W. Wei, H. Zhao, Z. Zhou, Y. Zhang, et al., Colorimetric detection of influenza A virus using antibody-functionalized gold nanoparticles, Analyst 140 (2015) 3989–3995.

[37] X. Wang, Y. Wei, S. Wang, L. Chen, Red-to-blue colorimetric detection of chromium via Cr (III)-citrate chelating based on Tween 20-stabilized gold nanoparticles, Colloids Surf. A Physicochem. Eng. Asp. 472 (2015) 57–62.

[38] J. Wei, L. Zheng, X. Lv, Y. Bi, W. Chen, W. Zhang, et al., Analysis of influenza virus receptor specificity using glycan-functionalized gold nanoparticles, ACS Nano 8 (2014) 4600–4607.

[39] M. Zhang, G. Qing, C. Xiong, R. Cui, D.W. Pang, T. Sun, Dual-responsive gold nanoparticles for colorimetric recognition and testing of carbohydrates with a dispersion-dominated chromogenic process, Adv. Mater. 25 (2013) 749–754.

[40] X. Zhang, H. Zhao, Y. Xue, Z. Wu, Y. Zhang, Y. He, et al., Colorimetric sensing of clenbuterol using gold nanoparticles in the presence of melamine, Biosens. Bioelectron. 34 (2012) 112–117.

[41] G. Zhou, Y. Liu, M. Luo, Q. Xu, X. Ji, Z. He, Peptide-capped gold nanoparticle for colorimetric immunoassay of conjugated abscisic acid, ACS Appl. Mater. Interfaces 4 (2012) 5010–5015.

[42] X. Sun, T. Chen, S. Huang, L. Li, H. Peng, Chromatic polydiacetylene with novel sensitivity, Chem. Soc. Rev. 39 (2010) 4244–4257.

[43] E. Lebegue, C. Farre, C. Jose, J. Saulnier, F. Lagarde, Y. Chevalier, et al., Responsive polydiacetylene vesicles for biosensing microorganisms, Sensors Basel (Basel) 18 (2018) 599–619.

[44] M.A. Reppy, B.A. Pindzola, Biosensing with polydiacetylene materials: structures, optical properties and applications, Chem. Commun. (Camb.) (2007) 4317–4338.

[45] Y.K. Jung, T.W. Kim, J. Kim, J.-M. Kim, H.G. Park, Universal colorimetric detection of nucleic acids based on polydiacetylene (PDA) liposomes, Adv. Funct. Mater. 18 (2008) 701–708.

[46] Y.K. Jung, H.G. Park, Colorimetric detection of clinical DNA samples using an intercalator-conjugated polydiacetylene sensor, Biosens. Bioelectron. 72 (2015) 127–132.

[47] Y.K. Jung, H.G. Park, J.M. Kim, Polydiacetylene (PDA)-based colorimetric detection of biotin-streptavidin interactions, Biosens. Bioelectron. 21 (2006) 1536–1544.

[48] D.-E. Wang, Y. Wang, C. Tian, L. Zhang, X. Han, Q. Tu, et al., Polydiacetylene liposome-encapsulated alginate hydrogel beads for Pb2+ detection with enhanced sensitivity, J. Mater. Chem. A Mater. Energy Sustain. 3 (2015) 21690–21698.

[49] E. Cho, S. Jung, Biomolecule-functionalized smart polydiacetylene for biomedical and environmental sensing, Molecules 23 (2018) 107–121.

[50] D.H. Kang, H.S. Jung, J. Lee, S. Seo, J. Kim, K. Kim, et al., Design of polydiacetylene-phospholipid supramolecules for enhanced stability and sensitivity, Langmuir 28 (2012) 7551–7556.

[51] E. Lebegue, C. Farre, C. Jose, J. Saulnier, F. Lagarde, Y. Chevalier, et al., Responsive polydiacetylene vesicles for biosensing microorganisms, Sensors Basel (Basel) 18 (2018).

[52] M.C. Lim, Y.J. Shin, T.J. Jeon, H.Y. Kim, Y.R. Kim, Microbead-assisted PDA sensor for the detection of genetically modified organisms, Anal. Bioanal. Chem. 400 (2011) 777–785.

[53] A. Pevzner, S. Kolusheva, Z. Orynbayeva, R. Jelinek, Giant chromatic Lipid/Polydiacetylene vesicles for detection and visualization of membrane interactions, Adv. Funct. Mater. 18 (2008) 242–247.

[54] S. Seo, J. Lee, E.-J. Choi, E.-J. Kim, J.-Y. Song, J. Kim, Polydiacetylene liposome microarray toward influenza a virus detection: effect of target size on turn-on signaling, Macromol. Rapid Commun. 34 (2013) 743–748.

[55] T. Eaidkong, R. Mungkarndee, C. Phollookin, G. Tumcharern, M. Sukwattanasinitt, S. Wacharasindhu, Polydiacetylene paper-based colorimetric sensor array for vapor phase detection and identification of volatile organic compounds, J. Mater. Chem. 22 (2012) 5970.

[56] H. Jeon, J. Lee, M.H. Kim, J. Yoon, Polydiacetylene-based electrospun fibers for detection of HCl gas, Macromol. Rapid Commun. 33 (2012) 972–976.

[57] J. Lee, S. Seo, J. Kim, Colorimetric detection of warfare gases by polydiacetylenes toward equipment-free detection, Adv. Funct. Mater. 22 (2012) 1632–1638.

[58] X. Wang, X. Sun, P.A. Hu, J. Zhang, L. Wang, W. Feng, et al., Colorimetric sensor based on self-assembled Polydiacetylene/Graphene-Stacked composite film for vapor-phase volatile organic compounds, Adv. Funct. Mater. 23 (2013) 6044–6050.

[59] S. Seo, J. Lee, M.S. Kwon, D. Seo, J. Kim, Stimuli-responsive matrix-assisted colorimetric water Indicator of polydiacetylene nanofibers, ACS Appl. Mater. Interfaces 7 (2015) 20342–20348.

[60] S. Seo, M.S. Kwon, A.W. Phillips, D. Seo, J. Kim, Highly sensitive turn-on biosensors

by regulating fluorescent dye assembly on liposome surfaces, Chem. Commun. (Camb.) 51 (2015) 10229–10232.
[61] D. Seo, J. Kim, Effect of the molecular size of Analytes on polydiacetylene chromism, Adv. Funct. Mater. 20 (2010) 1397–1403.
[62] J. Lee, M. Pyo, S.H. Lee, J. Kim, M. Ra, W.Y. Kim, et al., Hydrochromic conjugated polymers for human sweat pore mapping, Nat. Commun. 5 (2014) 3736.
[63] M. Wei, J. Liu, Y. Xia, F. Feng, W. Liu, F. Zheng, A polydiacetylene-based fluorescence assay for the measurement of lipid membrane affinity, RSC Adv. 5 (2015) 66420–66425.
[64] J. Lee, S. Seo, J. Kim, Rapid light-driven color transition of novel photoresponsive polydiacetylene molecules, ACS Appl. Mater. Interfaces 10 (2018) 3164–3169.
[65] G. Ma, Q. Cheng, Vesicular polydiacetylene sensor for colorimetric signaling of bacterial pore-forming toxin, Langmuir 21 (2005) 6123–6126.
[66] G.N. Patel, J.D. Witt, Y.P. Khanna, Thermochromisms in polydiacetylene solutions, J. Polym. Sci. 18 (1980) 1383–1391.
[67] J.-p. Jeong, E. Cho, D. Yun, T. Kim, I.-S. Lee, S. Jung, Label-free colorimetric detection of influenza antigen based on an antibody-polydiacetylene conjugate and its coated polyvinylidene difluoride membrane, Polymers 9 (2017) 127.
[68] J.-M. Kim, S.K. Chae, Y.B. Lee, J.-S. Lee, G.S. Lee, T.-Y. Kim, et al., Polydiacetylene supramolecules embedded in PVA film for strip-type chemosensors, Chem. Lett. 35 (2006) 560–561.
[69] J.-M. Kim, E.-K. J, S.M. Woo, H. Lee, D.J. Ahn, Immobilized polydiacetylene vesicles on solid substrates for use as chemosensors, Adv Mater 15 (2003) 1118–1121.
[70] C.H. Park, J.P. Kim, S.W. Lee, N.L. Jeon, P.J. Yoo, S.J. Sim, A. Direct, Multiplex biosensor platform for pathogen detection based on cross-linked polydiacetylene (PDA) supramolecules, Adv. Funct. Mater. 19 (2009) 3703–3710.
[71] Y. Scindia, L. Silbert, R. Volinsky, S. Kolusheva, R. Jelinek, Colorimetric detection and fingerprinting of Bacteria by glass-supported lipid-polydiacetylene films, Langmuir 23 (2007) 4682–4687.
[72] J.T. Wen, K. Bohorquez, H. Tsutsui, Polydiacetylene-coated polyvinylidene fluoride strip aptasensor for colorimetric detection of zinc(II), Sens. Actuators B Chem. 232 (2016) 313–317.
[73] D. Saviello, E. Pouyet, L. Toniolo, M. Cotte, A. Nevin, Synchrotron-based FTIR microspectroscopy for the mapping of photo-oxidation and additives in acrylonitrile-butadiene-styrene model samples and historical objects, Anal. Chim. Acta 843 (2014) 59–72.
[74] C.B. Casati, V. Sánchez, R. Baeza, N. Magnani, P. Evelson, M.C. Zamora, Relationships between colour parameters, phenolic content and sensory changes of processed blueberry, elderberry and blackcurrant commercial juices, Int. J. Food Sci. Technol. 47 (2012) 1728–1736.
[75] K.H. Bak, G. Lindahl, A.H. Karlsson, E. Lloret, G. Ferrini, J. Arnau, et al., High pressure effect on the color of minced cured restructured ham at different levels of drying, pH, and NaCl, Meat Sci. 90 (2012) 690–696.
[76] M. Abid, S. Jabbar, T. Wu, M.M. Hashim, B. Hu, S. Lei, et al., Effect of ultrasound on different quality parameters of apple juice, Ultrason. Sonochem. 20 (2013) 1182–1187.
[77] D.H. Kang, H.S. Jung, N. Ahn, J. Lee, S. Seo, K.Y. Suh, et al., Biomimetic detection of aminoglycosidic antibiotics using polydiacetylene-phospholipids supramolecules, Chem. Commun. (Camb.) 48 (2012) 5313–5315.
[78] G. Cuoco, C. Mathe, P. Archier, C. Vieillescazes, Characterization of madder and garancine in historic French red materials by liquid chromatography-photodiode array detection, J. Cult. Herit. 12 (2011) 98–104.
[79] N. Singh, S.M. Husson, B. Zdyrko, I. Luzinov, Surface modification of microporous PVDF membranes by ATRP, J. Membr. Sci. 262 (2005) 81–90.
[80] C. Zhao, G. Zhang, X. Xu, F. Yang, Y. Yang, Rapidly self-assembled polydopamine coating membranes with polyhexamethylene guanidine: formation, characterization and antifouling evaluation, Colloids Surf. A Physicochem. Eng. Asp. 512 (2017) 41–50.
[81] Z. Wang, J. Jin, D. Hou, S. Lin, Tailoring surface charge and wetting property for robust oil-fouling mitigation in membrane distillation, J. Membr. Sci. 516 (2016) 113–122.
[82] D.H. Park, J.M. Heo, W. Jeong, Y.H. Yoo, B.J. Park, J.M. Kim, Smartphone-based VOC sensor using colorimetric polydiacetylenes, ACS Appl. Mater. Interfaces 10 (2018) 5014–5021.
[83] F. Li, H. Li, Z. Wang, J. Wu, W. Wang, L. Zhou, et al., Mobile phone mediated point-of-care testing of HIV p24 antigen through plastic micro-pit array chips, Sens. Actuators B Chem. 271 (2018) 189–194.
[84] M. Bouscambert, M. Valette, B. Lina, Rapid bedside tests for diagnosis, management, and prevention of nosocomial influenza, J. Hosp. Infect. 89 (2015) 314–318.